J Supercond Nov Magn (2018) 31:989–993
DOI 10.1007/s10948-017-4285-0

ORIGINAL PAPER

# Enhancement of Critical Current Density of $MgB_2$ by Glutaric Acid Doping: a Simultaneous Improvement on the Intrinsic and Extrinsic Properties

**Jafar M. Parakkandy[1] · M. Aslam Manthrammel[2] · Fahad Saad Alghamdi[3] · Mohammed Shahabuddin[2] · Nasser S. Alzayed[2]**

Received: 30 May 2017 / Accepted: 2 August 2017 / Published online: 14 August 2017


**Abstract** In this study, we report an enhancement of critical current density of bulk $MgB_2$ superconductors by glutaric acid ($C_5H_8O_4$) doping. The effects of glutaric acid doping on $MgB_2$ lattice resulted in a record self-field $J_c$ of the order of $10^6$ A/cm$^2$. A simultaneous improvement in the connectivity, pinning force, and $H_{c2}$ is the major factor that determined excellent $J_c$ performance. X-ray diffraction analysis showed that samples were single-phase $MgB_2$ with a minor trace of impurities. A dramatic change in grain morphology and homogeneity in grain distribution was found in the SEM images of doped samples. We observed that homogeneity in grain distribution played a crucial role in the connectivity and the upper critical field ($H_{c2}$) of the doped samples. We were able to introduce a new dopant through a two-step mixing approach which is suitable to overcome the degradation of low field and self-field $J_c$ reported for carbon-doped $MgB_2$ superconductor samples.

**Keywords** $MgB_2$ superconductor · Glutaric acid doping · Critical current density · Upper critical field

✉ Jafar M. Parakkandy
j.parakkandy@psau.edu.sa

[1] Department of Physics, College of Science and Humanity Studies, Prince Sattam bin Abdulaziz University, Alkharj 11942, Kingdom of Saudi Arabia

[2] Department of Physics and Astronomy, College of Science, King Saud University, Riyadh 11451, Kingdom of Saudi Arabia

[3] National Center for Nanotechnology, King Abdulaziz City for Science and Technology, Riyadh, Kingdom of Saudi Arabia

## 1 Introduction

The 39 K [1] superconductor $MgB_2$ has been made significant enhancement by a lot of researches in the last decades. In particular, carbon substitution on B sites by a chemical reaction route [2–4] has proven the enhancement of $J_c$ under magnetic field. However, the homogenous mixing is still remaining as a challenge using any method. To overcome these difficulties to enhance the uniform dispersion of the C with B, various nanoparticles and materials including metallic elements having C in various forms like nanopowders, nanotubes, graphite, diamond, carbides, silicides, nitrides, borides, oxides, and hydrocarbons have been introduced into $MgB_2$ [5–15]. Among the C-containing dopants, Dou's group has achieved record performance in $MgB_2$ by SiC doping [4, 16]. Though many groups have reported similar results afterwards [16–19], the self-field and low-field performance has not improved much with SiC. A neutron diffraction study confirmed that most likely the solubility of carbon in $MgB_2$ is up to around 10% of C in the B sites, resulting in a large drop of critical temperature ($T_c$) and the $a$-axis parameter [20]. In order to overcome agglomeration of nano-additives in the precursors and to achieve homogeneous distribution of a small amount of nanodopants within the matrix, researchers proposed to use carbohydrate as a dopant and they explained many advantages of carbohydrate doping via chemical solution route method [23]. Many carbohydrates have been doped by different groups [21–23]. Among the carbohydrates, malic acid doping via chemical solution process has become popular and advantageous in terms of both cost and performance [24, 25]. Even though the malic acid doping is successful at high-field performance, they still have a problem with low-field degradation and inhomogeneity in substitution. In order to overcome this issue, in the present study, we report glutaric

acid ($C_5H_8O_4$) as a carbohydrate dopant for the first time via two-step wet mixing approach for the enhancement of low-field $J_c$. The organic dopant glutaric acid ($C_5H_8O_4$) melts at 98 °C but decomposes at 302 °C. Here, we perform a pre-heat treatment for the boron/dopant/toluene slurry at 120 °C. The pre-heat treatment helps the B to be coated with the dopant, thereby preventing the agglomeration and deterioration of B. We believe that this process provides better connectivity and enhanced low-field $J_c$ for the sample. Further, we confirmed from our results that these organic compounds have a potential to improve physical properties of $MgB_2$ for low-field application like MRI.

## 2 Experimental Procedure

$MgB_2$ bulk samples were synthesized by an *in-situ* reaction process. In the present study, the amount of glutaric acid dopants was selected such that it substitutes 2 to 8 at.% of carbon into $MgB_2$ lattice. An appropriate amount of dopant was taken in an 80 ml bowl having 10 ml of toluene solution ($C_7H_8$, 99.5%). A stoichiometric amount of amorphous nano-boron (PVZ nano Boron, Pavezyum) was then added into it. This mixture was ball milled with six $ZrO_2$ balls of 5 mm diameter for 2 h with 100 rpm speed. This slurry mixture was dried in an oven at 120 °C for 15 h, so that the B powder particles were coated by the dopant uniformly. This uniform composite was then mixed with an appropriate amount of 99.9% Mg powder (CERAC with an average particle size of 45 µm, −325 mesh) and grounded for 20 min by an agate mortar and pestle. The samples were then pelletized under 10 tons of pressure. All pellets were wrapped with a tantalum foil and heat treated at 650 °C for 2 h in high-purity argon atmosphere (with a heating rate of 5 °C/min to reach a temperature of 650 °C).

## 3 Results and Discussion

Figure 1 shows the powder XRD patterns of the samples. $MgB_2$, the major phase, and a trace amount of MgO and unreacted Mg phases were observed. Rietveld refinement was performed to analyze the XRD data. It shows the increase of MgO percentage with an increase of doping level. This increase is obvious due to the increase of oxygen amount with the increase of the doping percentage level.

Figure 2 shows a sequential reduction in the $a$-lattice parameter and the actual amount of C substitution in $Mg(B_{1-x}C_x)_2$, calculated from the $c/a$ ratio using $x = 7.5 \times \Delta(c/a)$ [26] as a function of glutaric acid doping level. The graph clearly indicates that the value of $x$ is less than the actual doping percentage. This shows a partial substitution of C in $MgB_2$ and a partial diffusion into the

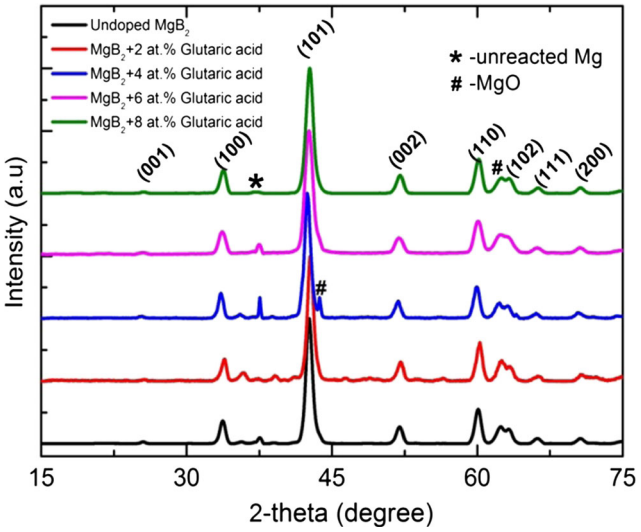


**Fig. 1** XRD spectrum of glutaric acid-doped $MgB_2$ for different doping percentages

$MgB_2$ matrix as an interstitial atom. The partial substitution of C in the present case is due to the low sintering temperature (650 °C). A higher sintering temperature around 900 °C may be needed to achieve the full substitution of C.

We studied the magnetic field dependence of $J_c$ of the doped and undoped samples at 5 and 20 K (as shown in Fig. 6). As we achieve the highest $J_c$ for the 6 at.% doped sample, we present the FE-SEM images of pure and 6 at.% glutaric acid-doped samples in Fig. 3 for microstructure comparison. There is a dramatic change in the grain morphology of the pure and doped samples. The grain morphology of pure sample is more or less spherical while that of the doped sample is in needle shape. Grains are more homogeneous and smaller in size in the doped one. This

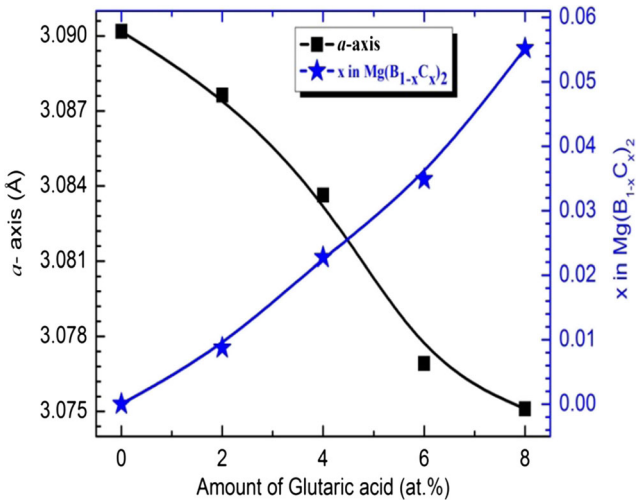


**Fig. 2** $a$-Lattice parameter and carbon substitution $x$ as a function of doping percentage of glutaric acid

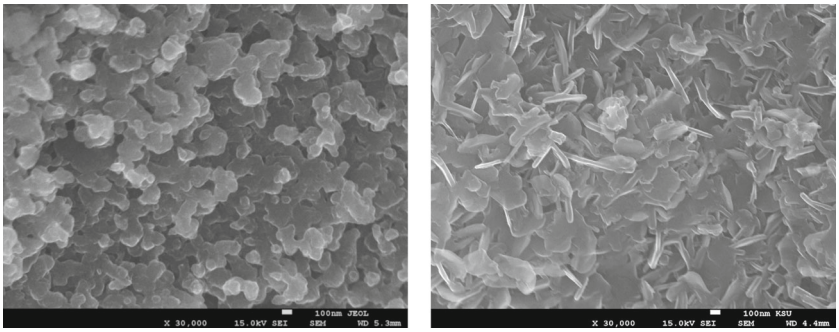


**Fig. 3** FE-SEM image of pure and 6 at.% glutaric acid-doped $MgB_2$

makes the sample relatively more compact and provides better connectivity. Further, the smaller and needle-shaped grain provides better pinning strength in the sample. To compare the connectivity in these samples, the normal-state resistivity measurements were carried out.

The connectivity factor ($A_f$) and residual resistivity ($\rho_0$) were calculated from the normal-state resistivity measurement. Strain in these samples was calculated from the Rietveld analysis using MAUD software. These results are shown in Fig. 4. The connectivity ($A_f$) of the samples was calculated by the equation proposed by Rowell [27]. There is a comparative increase in connectivity with doping. As we mentioned earlier, we expect the pre-heat treatment of boron-dopant slurry at 120 °C will produce a dopant-coated B which prevents the agglomeration and oxidation of B. Thus, we get the uniformly de-agglomerated dopant-coated B powder with high surface area. The dopant in this mixture is expected to decompose during the sintering process at 302 °C and release highly reactive C during the $MgB_2$ formation process, homogeneously throughout the sample. This homogeneity in distribution of dopant-coated B causes an increase in the percentage of connectivity which gives a better performance in low-field $J_c$. The residual resistivity ($\rho_0$) of the samples was calculated using the Rowell technique with an inter-grain connectivity correction ($\rho_0 = A_f \times \rho_{40\,K}$), as explained elsewhere [28]. The residual resistivity of the samples is increased with doping percentage. The partial C substitution and distortion in the B-plane are the causes of the scattering of the electrons taking part in the transport of the current, and hence, we observe an increase in the residual resistivity. The increase in lattice stain is expected due to the increase in partial C substitution and the decrease in crystallinity in the sample as discussed earlier. It is argued that the decrease in grain size, the increase in MgO, and the partial carbon substitution are the main causes of the distortion in the $MgB_2$ lattice structure resulting in the lattice strain [29, 30]. The increased impurity scattering due to partial C substitution obviously enhances the $H_{c2}$ of the sample. $H_{c2}(T)$ has been calculated from the field-dependent $R$–$T$ plots using the criteria of 90% of normal state resistivity as shown in Fig. 5.

The $H_{c2}$ shows the enhancement with doping at all temperatures. In order to get an estimated value of $H_{c2}(0)$, we

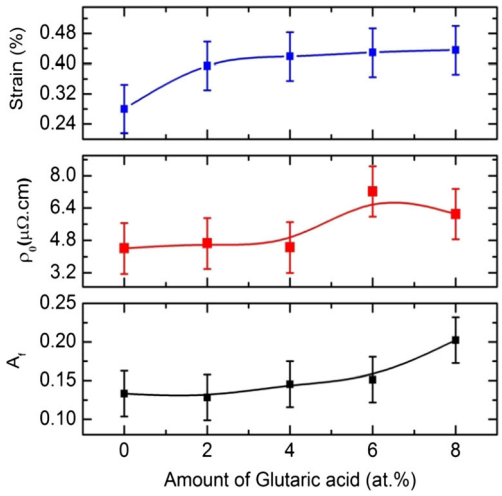


**Fig. 4** Connectivity factor ($A_f$), residual resistivity ($\rho_0$), and strain as a function of atomic percent of glutaric acid

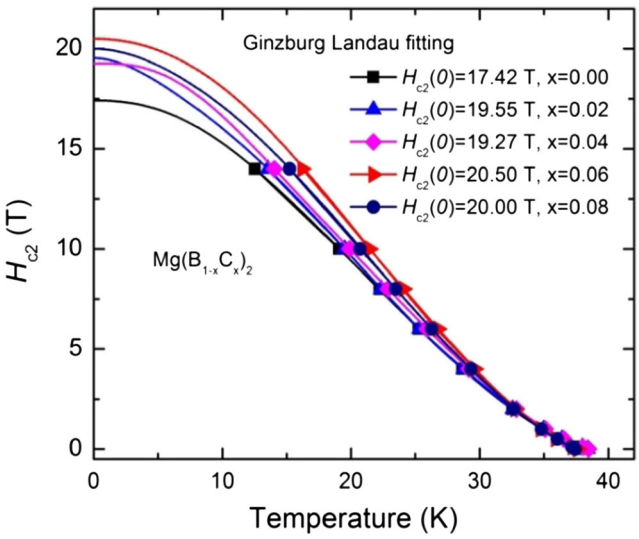


**Fig. 5** Theoretically fitted curves for $H_{c2}$ vs temperature plots for pure and glutaric acid-doped $MgB_2$ superconductors

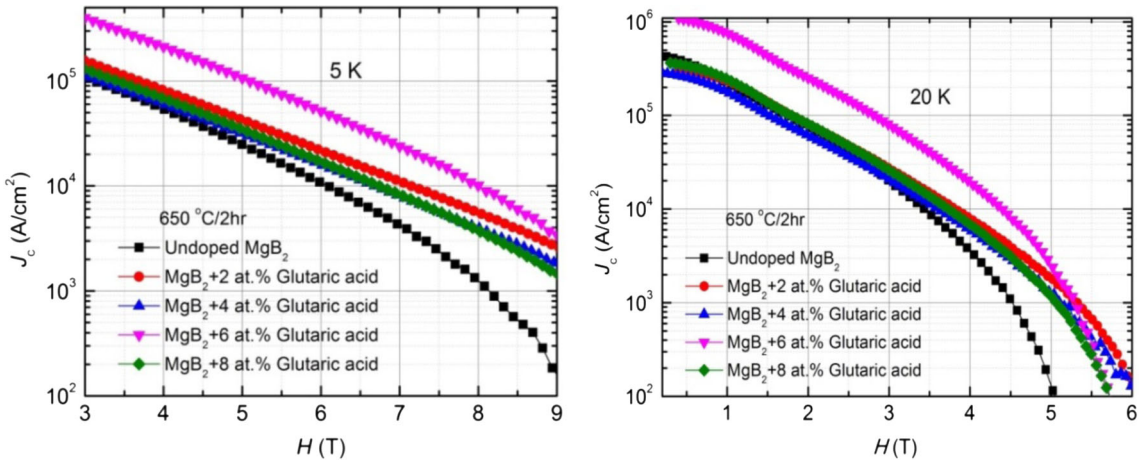


**Fig. 6** $J_c(H, T)$ of pure and glutaric acid-doped $MgB_2$ samples at 5 and 20 K

have used the Ginsburg-Landau theory [31]. Both experimental and fitted curves for $H_{c2}$ are shown in Fig. 5. The fitted curves are in solid line, while experimental data points are shown by a symbol. We observed that $H_{c2}(0)$ increased from 17.4 T for the undoped samples to 20.5 T for the 6 at.% glutaric acid-doped sample. This increase in $H_{c2}(T)$ is remarkably helpful to enhance the high-field $J_c$ $(H)$. This needs an electromagnetic study to investigate in detail.

Figure 6 shows magnetic field dependence of $J_c$ of the doped and undoped samples at 5 and 20 K. As can be seen in the figure, self-field $J_c$ at 20 K for the 6 at.% doped sample is of the order of $10^6$ A/cm$^2$. In the low-field region, i.e., at 20 K and 4 T field, the $J_c$ value enhanced from $3.5 \times 10^3$ A/cm$^2$ for the pure sample to $1.93 \times 10^4$ A/cm$^2$ for the 6 at.% doped samples. The enhancement in $J_c$ at 20 K and 4 T is highly useful for cryogen-free operation of superconducting MRI magnets. The enhancement of $J_c$ in the low-field region with glutaric acid doping is the highest compared to all the other dopants so far in bulk samples. Connectivity, pinning force, and $H_{c2}$ determine the $J_c(H, T)$ behavior of superconducting materials. The enhancement in $J_c$ is directly proportional to grain connectivity and pinning forces. We have seen from the resistivity studies that the connectivity of the sample is increased substantially with doping as shown in Fig. 4. We calculated the pinning force using the formula $F_p = \mu_0 H \times J_c$ from the $J_c$–$H$ data.

The pinning forces at 20 K temperature are shown in Fig. 7. From Fig. 7, it is clearly seen that the pinning force ($F_p$) is increasing with increasing doping percentage. The pinning force is highest for the 6 at.% doped sample. The increased pinning force is due to the smaller grain size in the doped sample which was evident from the XRD analysis and SEM images as discussed before. Martinez et al. [32] observed that the pinning force maxima ($F_{pmax}$) increases with the decrease in grain size for the samples having good grain connectivity. This behavior is also present in our present study. The maximum self-field and low-field $J_c(H, T)$ observed in the 6 at.% doped sample is due to the increase in connectivity and pinning force.

In low temperature and high field, i.e., at 5 K and 8 T field, the $J_c$ value enhanced from $1.23 \times 10^3$ A/cm$^2$ for the pure sample to $1.0 \times 10^4$ A/cm$^2$ for the 6 at.% doped samples. Under high-field $J_c$, the 6 at.% doped sample obviously shows superior properties. The high-field $J_c$ enhancement is generally governs by the $H_{c2}$ and pinning force. We have seen from the resistivity study that $H_{c2}$ of the sample has increased with doping percentage. The maximum $H_{c2}$ is observed for the 6 at.% doped samples. As discussed before, the enhancement in $H_{c2}$ is mainly due to impurity scattering in the sample. We have seen from the XRD studies that doping causes a partial substitution of C in $MgB_2$ as well as partial diffusion of C into the $MgB_2$ matrix as an interstitial atom. This partial C substitution

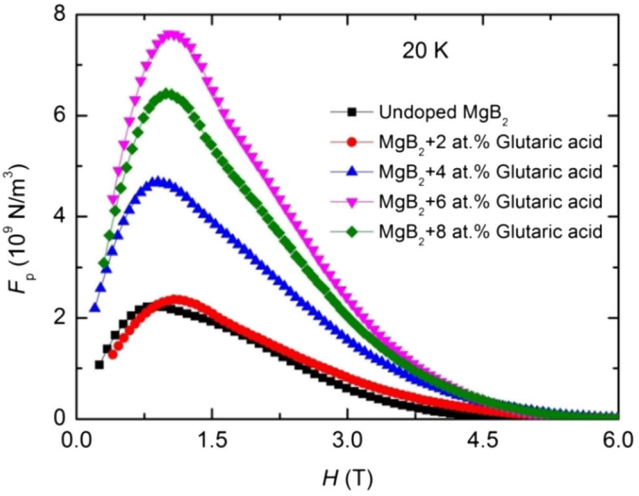


**Fig. 7** $F_p$–$H$ characteristics of glutaric acid-doped and pure $MgB_2$ superconductors at 20 K

and distortion in the B-plane enhance the electron scattering and thereby cause an increase in the residual resistivity. The increased electron scattering in B-plane results in a decrease in mean free path and hence larger $H_{c2}$ and hence $J_c$ in the sample. The second factor, which governs the high-field $J_c$, is the pinning force. We already discussed that the pinning force ($F_p$) is increasing with doping percentage and the maximum pinning force is observed for the 6 at.% doped sample. The pinning force enhancement causes an increase in irreversibility field and hence enhancement in $J_c$. These results suggest that the high-field $J_c$ enhancement is due to enhanced $H_{c2}$ and pinning force.

## 4 Conclusion

In summary, we studied the effect of glutaric acid ($C_5H_8O_4$) doping on the structural and superconducting properties of $MgB_2$ superconductors. Simultaneous improvements of intrinsic and extrinsic properties of $MgB_2$ were observed with glutaric acid ($C_5H_8O_4$) doping. The calculated actual amount of C substitution clearly indicates that a partial substitution of C in $MgB_2$ and a partial diffusion into the $MgB_2$ matrix as an interstitial atom are due to the low sintering temperature (650 °C). Grain morphology showed a dramatic change in shape and homogeneity in grain distribution with doping. The connectivity and the upper critical field ($H_{c2}$) of the doped samples increased significantly and reflected in the $J_c$ values. A recorded self-field $J_c(0)$ value of the order of $10^6$ A/cm$^2$ was obtained for the 6 at.% glutaric acid-doped sample. The connectivity, pinning force strength, and $H_{c2}$ determined the excellent performance of critical current density. We have optimized the dispersion and percentage of the glutaric acid doping which has given the best performance of electromagnetic properties.

**Acknowledgements** The authors would like to extend their sincere appreciation to the Deanship of Scientific Research at King Saud University for the funding of this research through the Research Group Project No. RGP-290.

## References

1. Nagamatsu, J., Nakagawa, N., Muranaka, T., et al.: Nature **410**, 63–64 (2001)
2. Dou, S.X., Shcherbakova, O., Yeoh, W.K., et al.: Phys. Rev. Lett. **98**, 130404 (2007)
3. Wang, J.L., Zeng, R., Kim, J.H., et al.: Phys. Rev. B **77**, 174501 (2008)
4. Dou, S.X., Soltanian, S., Horvat, J., et al.: Appl. Phys. Lett. **81**, 3419–3421 (2002)
5. Barua, S., Patel, D., Alzayed, N., et al.: Mater. Lett. **139**, 333–335 (2015)
6. Collings, E.W., Sumption, M.D., Bhatia, M., et al.: Supercond. Sci. Tech. **21**, 103001 (2008)
7. Eisterer, M.: Supercond. Sci. Tech. **20**, R47–R73 (2007)
8. Ansari, I.A., Parakkandy, J.M., Shahabuddin Shah, M., et al.: Arab. J. Sci. Eng. **42**, 383–388 (2017)
9. Dou, S.X., Soltanian, S., Yeoh, W.K., et al.: IEEE Trans. Appl. Supercond. **15**, 3219–3222 (2005)
10. Dou, S.X., Shcherbakova, O., Yoeh, W.K., et al.: Phys. Rev. Lett. **98**, 097002 (2007)
11. Yeoh, W.K., Dou, S.: Physica C **456**, 170–179 (2007)
12. Bhatia, M., Sumption, M.D., Collings, E.W.: IEEE T. Appl. Supercon. **15**, 3204–3206 (2005)
13. Shahabuddin Shah, M., Shahabuddin, M., Parakkandy, J.M., et al.: Solid State Commun. **218**, 31–34 (2015)
14. Alzayed, N.S., Soltan, S., Shahabuddin, M., et al.: J. Supercond. Nov. Magn. **28**, 387–390 (2015)
15. Patel, D., Maeda, M., Choi, S., et al.: Scripta Mater. **88**, 13–16 (2014)
16. Dou, S.X., Braccini, V., Soltanian, S., et al.: J. Appl. Phys. **96**, 7549–7555 (2004)
17. Kumakura, H., Kitaguchi, H., Matsumoto, A., et al.: Appl. Phys. Lett. **84**, 3669–3671 (2004)
18. Sumption, M.D., Bhatia, M., Rindfleisch, M., et al.: Appl. Phys. Lett. **86**, 092507 (2005)
19. Yamamoto, A., Shimoyama, J., Ueda, S., et al.: Supercond. Sci. Tech. **18**, 1323–1328 (2005)
20. Singh, P.P.: Solid State Commun. **127**, 271–274 (2003)
21. Parakkandy, J.M., Shahabuddin, M., Shah, M.S., et al.: J. Supercond. Nov. Magn. **28**, 475–479 (2015)
22. Ghorbani, S.R., Darini, M., Wang, X.L., et al.: Solid State Commun. **168**, 1–5 (2013)
23. Kim, J.H., Zhou, S., Hossain, M.S.A., et al.: Appl. Phys. Lett. **89**, 142505 (2006)
24. Kim, J.H., Dou, S.X., Hossain, M.S.A., et al.: Supercond. Sci. Tech. **20**, 715–719 (2007)
25. Hossain, M.S.A., Kim, J.H., Xu, X., et al.: Supercond. Sci. Tech. **20**, L51–L54 (2007)
26. Avdeev, M., Jorgensen, J.D., Ribeiro, R.A., et al.: Physica C **387**, 301–306 (2003)
27. Rowell, J.: M. Supercond. Sci. Tech. **16**, R17–R27 (2003)
28. Shahabuddin, M., Alzayed, N.S., Jafar, M.P., et al.: Physica C **471**, 1635–1642 (2011)
29. Kim, J.H., Dou, S.X., Oh, S., et al.: J. Appl. Phys. **104**, 063911 (2008)
30. Kim, J.H., Oh, S., Heo, Y.U., et al.: Npg Asia Mater. **4**, 2945–2986 (2012)
31. Askerzade, I.: N. Phys-Usp+ **49**, 1003–1016 (2006)
32. Martinez, E., Mikheenko, P., Martinez-Lopez, M., et al.: Phys. Rev. B **75**, 134515 (2007)